

Lattice dynamics of fcc and bcc calcium

M. Heiroth,* U. Buchenau, and H. R. Schober

Institut für Festkörperforschung der Kernforschungsanlage Jülich, Postfach 1913, D-5170 Jülich, West Germany

J. Evers

Institut für Anorganische Chemie, Universität München, Meiserstrasse 1, D-8000 München 2, West Germany

(Received 6 May 1986)

The phonon-dispersion curves of Ca in the fcc and bcc phase have been derived from inelastic-neutron-scattering measurements of polycrystalline samples. The elastic constants were determined from the low-frequency part of the spectra. No pronounced softening of the elastic shear constants towards the martensitic phase transformation could be observed within the accuracy of the measurement. The high-frequency part of the neutron spectra was analyzed in terms of Born–von Kármán models and pseudopotential models. Even though pronounced phonon anomalies are absent in both phases, the results show that a simple pseudopotential picture is inadequate.

I. INTRODUCTION

It is interesting to compare the lattice dynamics of one and the same element in two different structural modifications. The comparison provides a much more stringent test for simple phonon models than the phonon dispersion in a single structure. In this paper we report on measurements of the phonons of fcc and bcc calcium. The phonon dispersion has been determined from the coherent inelastic neutron scattering of a polycrystalline sample. Within this method the dynamical matrix is parametrized in terms of Born–von Kármán (BvK) models. The free parameters are determined by a fit to the inelastic time-of-flight spectrum which was measured over the entire ω range and in a Q range covering the first five to six inequivalent Brillouin zones. The method has been previously applied to Ba and Sr,¹ and to room-temperature Ca.² The reliability of these results was proved later by triple axis neutron measurements on fcc Ca and bcc Ba which agreed with maximum deviations of 10%.^{3,4} The method allows one to measure the same sample in the two different crystalline structures simply by recording the scattering at two temperatures just above and below the transition temperature (in the case of calcium the transition from the high-temperature bcc phase to the low-temperature fcc phase takes place at 721 K).

The question whether one can give a consistent description of the phonons in bcc and fcc calcium cannot be answered by a comparison of the Born–von Kármán parameters. The simplest scheme which allows the calculation of the phonons with the same parameters for both structures is a local pseudopotential.^{5,6} Though the applicability of this scheme to Ca is doubtful because of the proximity of the d band to the Fermi surface,^{5,7} it is still in use for Ca (Ref. 8) and its homologues (Ref. 9). Therefore, we extended the method to the use of local pseudopotential models. For our calculations we chose a model pseudopotential adequate for simple s - p metals.¹⁰ The re-

sults will be discussed and compared to those obtained with BvK models.

II. EXPERIMENTAL DETAILS

Calcium is a reactive metal. As a consequence, in commercial quality this metal can contain a lot of nonmetallic impurities, especially hydrogen and oxygen. For this investigation calcium was purified by ultrahigh-vacuum distillation. In order to avoid recontamination with nonmetallic impurities, the purified metal was always handled in a controlled atmosphere of argon. More details of the purification and handling procedure described below are reported elsewhere.¹¹ Calcium grains (purity with respect to metallic impurities > 99%) prepared by Koch-Light Laboratories, England, were used as starting material. The distillation was performed in a molybdenum crucible with a column of molybdenum foil which was outgassed at 1500°C at high-vacuum conditions before use. Calcium was distilled for 6 h with a temperature of 880°C at the bottom of the crucible and 700°C at the top of the column. The vacuum steadily increased to 10^{-8} mbar at the end of the distillation. After cooling, the distillation tube was transferred into the glove box where the slightly yellow colored calcium was cut from the molybdenum column.

The experiment was done on the time-of-flight spectrometer SV 5 at the cold source of the DIDO reactor at Jülich (wave vector of the incoming neutrons $k_i = 1.314$ Å, range of scattering angles 20°–160°). For the 100-K and room-temperature measurements, about 38 g Ca were sealed in a thin-walled aluminum container. For the high temperatures (680, 705, 726, and 750 K), we used a stainless-steel container. The 100-K measurement was done in a closed-cycle cryostat and the high-temperature measurement in a water-cooled furnace. In order to ensure a good orientational average, the samples were rotated around an axis perpendicular to the scattering plane during the measurement.

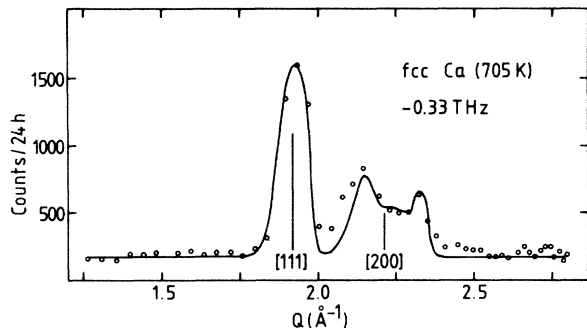


FIG. 1. Inelastic intensities obtained from polycrystalline fcc Ca between -0.22 and -0.45 THz (energy gain of the neutrons) at 705 K. The line is a fitted curve with the elastic constants of Table I.

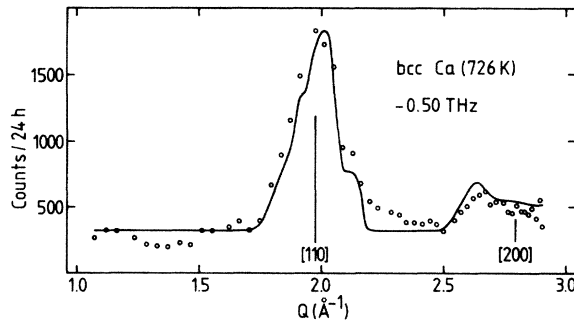


FIG. 2. Inelastic intensities obtained from polycrystalline bcc Ca between -0.29 and -0.54 THz (energy gain of the neutrons) at 726 K. The line is a fitted curve with the elastic constants of Table I.

III. RESULTS AND DISCUSSIONS

A. Elastic constants

The elastic constants $c' = (c_{11} - c_{12})/2$ and c_{44} for both structures of Ca were determined by fits to the low-frequency part of the spectra near the Debye-Scherrer rings¹² with an energy gain of the neutrons. Such fits are presented in Fig. 1 (705 K; fcc) and Fig. 2 (726 K; bcc). The resulting elastic constants are compiled in Table I.

As seen from Table I, the accuracy of the determination is highest for the smallest shear constant c' . This result is understandable, because a low transverse elastic shear constant leads to a high density of sound wave states and thus dominates the signal at low frequencies.

The values at room temperature are compared in Table I to the single-crystal results of Stassis *et al.*³ While c_{44} agrees with the single-crystal value within the accuracy of our measurement, there is a discrepancy in c' , our value being about 40% lower. We believe that our value of c' is more accurate than the one of Ref. 3. In their work, c' was taken from the Born-von Kármán fit of the measured frequencies. The elastic constant c' determines the slope of the T_2 branch along the [110] direction. From their lowest measured phonon frequency of that branch at

0.8 THz and at [0.20.20] in the reciprocal lattice, one calculates $c' = 3.8$ GPa, much closer to our value of 3.4 GPa than to their value of 4.8 GPa. Moreover, our measurement extends down to 0.2 THz, a factor of 4 lower than the single-crystal data. Since the branch has an anomalous dispersion, measurements at lower frequencies are expected to give more accurate results for its initial slope.

As seen from Table I, the elastic shear constant c' is fairly small in the fcc phase and in the bcc phase as well. In the limit of small deformations, c' provides the restoring force against the Bain deformation¹⁴ in both phases. The Bain deformation is a conceptually simple way to pass from the fcc to the bcc structure and vice versa by appropriate elongations and contractions along the cubic axes. Though the detailed mechanisms in real martensitic fcc-bcc transformations seem to be more complicated¹⁵ and are probably different in different systems, they involve as a rule a major shear strain component against the elastic constant c' . Thus the smallness of c' could be connected to the existence of two neighboring minima of the free energy in configuration space corresponding to the fcc and bcc structures. However, within our accuracy limits the temperature dependence of c' shows no anomalous features near the martensitic phase transfor-

TABLE I. Measured elastic constants of Ca.

Temperature (K)	$c' = \frac{1}{2}(c_{11} - c_{12})$ (GPa)	c_{44} (GPa)	c_{11} (GPa)
fcc Ca			
100	3.6 ± 0.3	15 ± 3	
300	3.4 ± 0.3 (4.79 ^a)	14 ± 3 (16.3 ^a)	22.8^b (27.8 ^a)
680	2.2 ± 0.2	10 ± 3	
705	2.2 ± 0.2	10 ± 3	
bcc Ca			
726	1.6 ± 0.2	12 ± 3	
750	1.6 ± 0.2	13 ± 3	

^aValues determined on single-crystal data (Ref. 3).

^b C_{11} has been calculated from $B_0 = 18.3$ GPa (Ref. 13).

TABLE II. Born–von Kármán force constants of Ca.

Neighbor and indices	Force constants (N/m)				Neighbor and indices	Force constants (N/m)	
	100 K	293 K	680 K	705 K		726 K	750 K
	fcc calcium					bcc calcium	
1xx	4.472	4.223	4.321	4.267	1xx	4.014	3.936
1zz	0.293	0.236	0.153	0.064	1xy	3.503	3.582
1xy	4.180	3.988	4.168	4.202	2xx	1.443	1.441
2xx	-1.000	-0.902	-0.472	-0.506	2xy	-1.182	-0.926
2yy	-0.112	-0.190	-0.430	-0.464	3xx	0.042	0.062
3xx	0.020	0.056	-0.040	-0.027	3zz	-0.108	-0.104
3yy	-0.042	-0.028	-0.069	-0.051	3xy	0.150	0.166
3yz	0.021	0.028	0.010	0.008			
3xz	0.041	0.056	0.020	0.016			

mation like those observed in fcc-fct transitions of In alloys.¹⁶ Especially there seems to be no increase of c' with increasing temperature above the martensitic transformation temperature.

B. Born–von Kármán fits

The measured data were corrected for self-absorption, multiple scattering, and for multiphonon contributions.¹⁷ The phonon dispersion curves were derived from fits of Born–von Kármán models to the experimental data between 0.3 and 6 THz. The BvK fits were done with the elastic constants as constraints (additional fits without constraints reproduced the phonons within 5% and the elastic constants within 10%). It turned out to be sufficient to use a simple axially symmetric model including the first three neighbor shells.

The obtained BvK parameters for all measured temperatures are given in Table II. The resulting phonon dispersion curves are shown in Fig. 3 (293 K; fcc) and Fig. 4 (726 K; bcc). Figure 3 compares our result at room temperature to the BvK fit of the single-crystal work.³ The overall agreement is very good. Significant differ-

ences occur only at the X and W points. From our experience with different BvK fits, we think that at these points the single-crystal values may be more accurate. The only anomalous feature is a positive dispersion in the T_2 branch in the $[110]$ direction (this is also found at the other temperatures and in the single-crystal measurements³). It has been suggested that this anomaly is caused by d -band hybridization.¹⁸

In the bcc case the T_2 branch in the $[110]$ direction is very low up to the zone boundary. However, no anomalous temperature dependence of the zone-boundary modes like that observed in Li (Ref. 19) and Na (Ref. 20) has been seen in either of the two phases of Ca, neither in the T_2 branch nor in any other branch. There are as yet no single-crystal results for bcc Ca. However, one can compare our results to measured phonons in bcc Sr (Ref. 21) and bcc Ba (Refs. 1 and 4) which show a general similarity to the curves reported here. It is especially interesting to compare the branches along $[100]$. In Ba, the longitudinal branch lies below the transverse branch,⁴ an anomaly which could be reproduced in frozen-phonon calculations by Chen *et al.*²² According to these authors, the anomaly is due to the influence of the empty d band

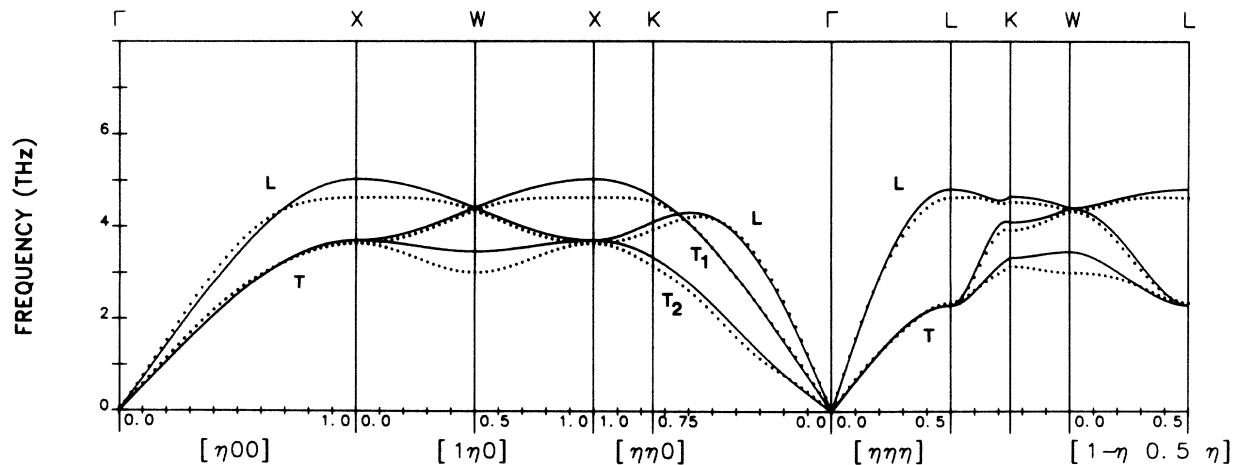


FIG. 3. Phonon dispersion curves of fcc Ca at 293 K: (—), third-neighbor axially symmetric Born–von Kármán fit to the polycrystalline neutron time-of-flight spectra; (· · ·), eighth-neighbor Born–von Kármán fit to single-crystal data (Ref. 3).

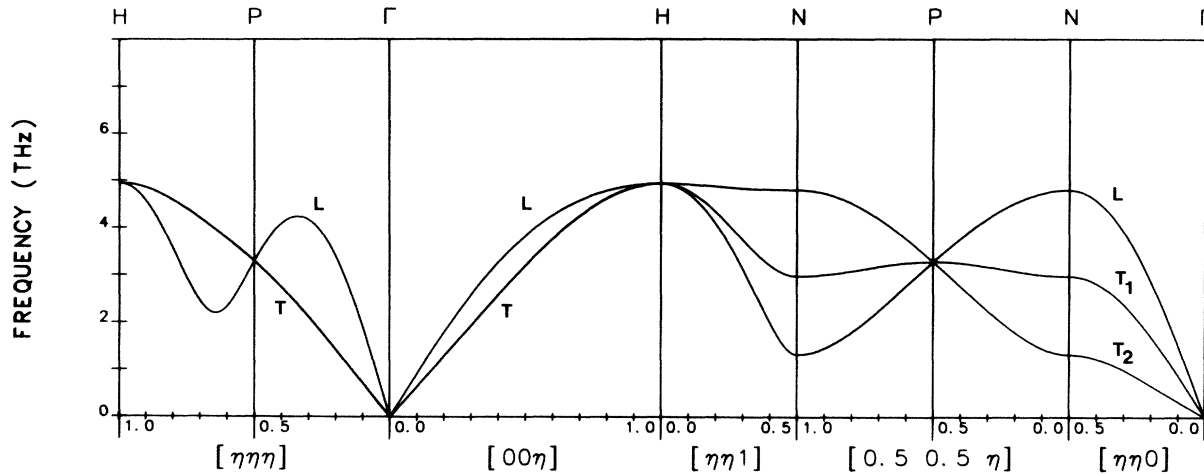


FIG. 4. Phonon dispersion curves of bcc Ca at 726 K. Third-neighbor axially symmetric Born–von Kármán fit to the polycrystalline neutron time-of-flight spectra.

lying very close above the Fermi surface. In bcc Sr (Ref. 21) and even more in our present data for bcc Ca, the branches shift back to their normal sequence. Following Chen *et al.*,²² this tendency can be understood in terms of an increasing distance between the empty *d* band and the Fermi surface going from Ba to Ca.

C. Comparison to calorimetric data

The vibrational density of states calculated²³ from the fit results is shown in Fig. 5 (fcc at 300 and 705 K) and in Fig. 6 (bcc at 726 K). The comparison of the two fcc density-of-states curves in Fig. 5 shows, on the average, a

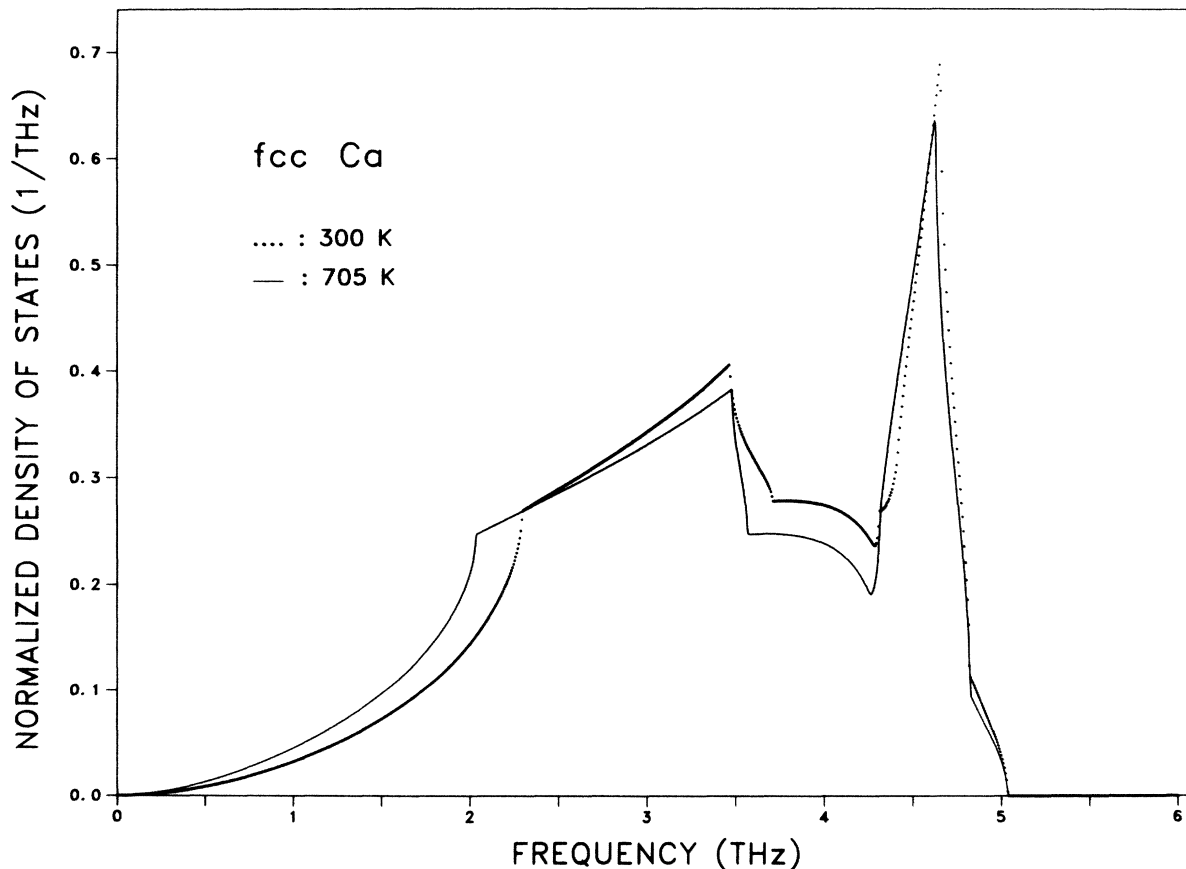


FIG. 5. Phonon spectrum of fcc Ca calculated with the Born–von Kármán parameters of Table II: (—), $T=300$ K; (· · · ·), $T=705$ K.

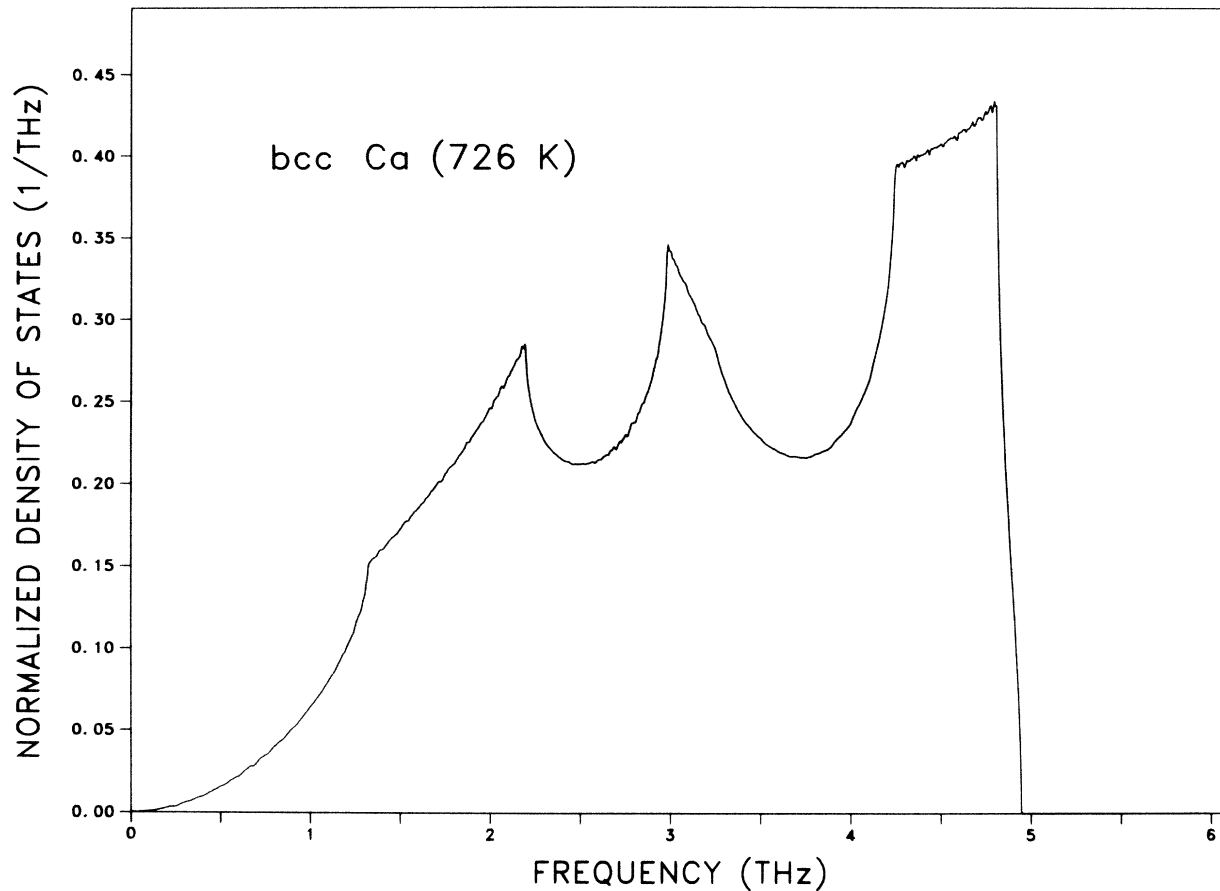


FIG. 6. Phonon spectrum of bcc Ca calculated with the Born–von Kármán parameters of Table II ($T = 726$ K).

decrease of the phonon frequencies with increasing temperature. This decrease leads to an excess term in the lattice specific heat over the harmonic Dulong-Petit value of $3Nk_B$ (N is the number of atoms per mole and k_B , the Boltzmann constant). In a quasiharmonic approximation²⁴ the specific heat is given by ($x = h\nu'/2k_B T$)

$$C_p = 3Nk_B \int_0^\infty d\nu' Z(\nu', T) \frac{x^2}{\sinh^2(x)} \left[1 - \left[\frac{\partial \langle \ln \nu \rangle}{\partial \ln T} \right]_p \right], \quad (1)$$

where

$$\langle \ln \nu \rangle = \int_0^\infty d\nu Z(\nu, T) \ln \nu \quad (2)$$

(ν is the frequency and $Z(\nu, T)$ the vibrational density of states at the temperature T). We assumed a linear dependence of $\langle \ln \nu \rangle$ between 300 and 705 K. Adding a linear electronic specific-heat term²⁵ with $\gamma_e = 0.003$ J/mol K², we obtained the calculated curve in Fig. 7, which is in good general agreement with the measured specific heat.²⁵ The comparison shows that the excess specific heat over the Dulong-Petit value can be understood in terms of the decrease of the phonon frequencies with increasing temperature. It seems to be unnecessary to invoke any anomaly in the electronic part of the specific heat.

In the bcc phase we have only measured at two tem-

peratures not very distant from each other. Therefore, it was not possible to determine the excess term of the specific heat as in the fcc case. What one can do is compare the vibrational part of the entropy in the two different phases. The vibrational entropy was calculated from this expression²⁴

$$S = 3Nk_B \int_0^\infty d\nu Z(\nu, T) \{ -\ln[2 \sinh(x)] + x \coth(x) \}, \quad (3)$$

where $x = h\nu/2k_B T$.

One finds an entropy difference of the two phases of 0.85 ± 0.2 J/K mole. The resulting difference in enthalpy at 721 K is 610 ± 150 J/mole (the pressure term in the enthalpy difference can be neglected because the atomic volume is practically the same in both phases²⁶). Within the error limits, this value agrees with the latent heat of 920 ± 200 J/mole found by calorimetric measurements.²⁵ This shows that the driving force for the phase transformation is indeed the vibrational entropy difference between fcc and bcc, which favors the bcc phase at higher temperatures.

It is interesting to compare the enthalpy difference and the calculated energy differences between fcc and bcc phases at 0 K. In principle, these values should be the same, if one assumes that different temperature effects on the electronic ground-state energies are the same in both

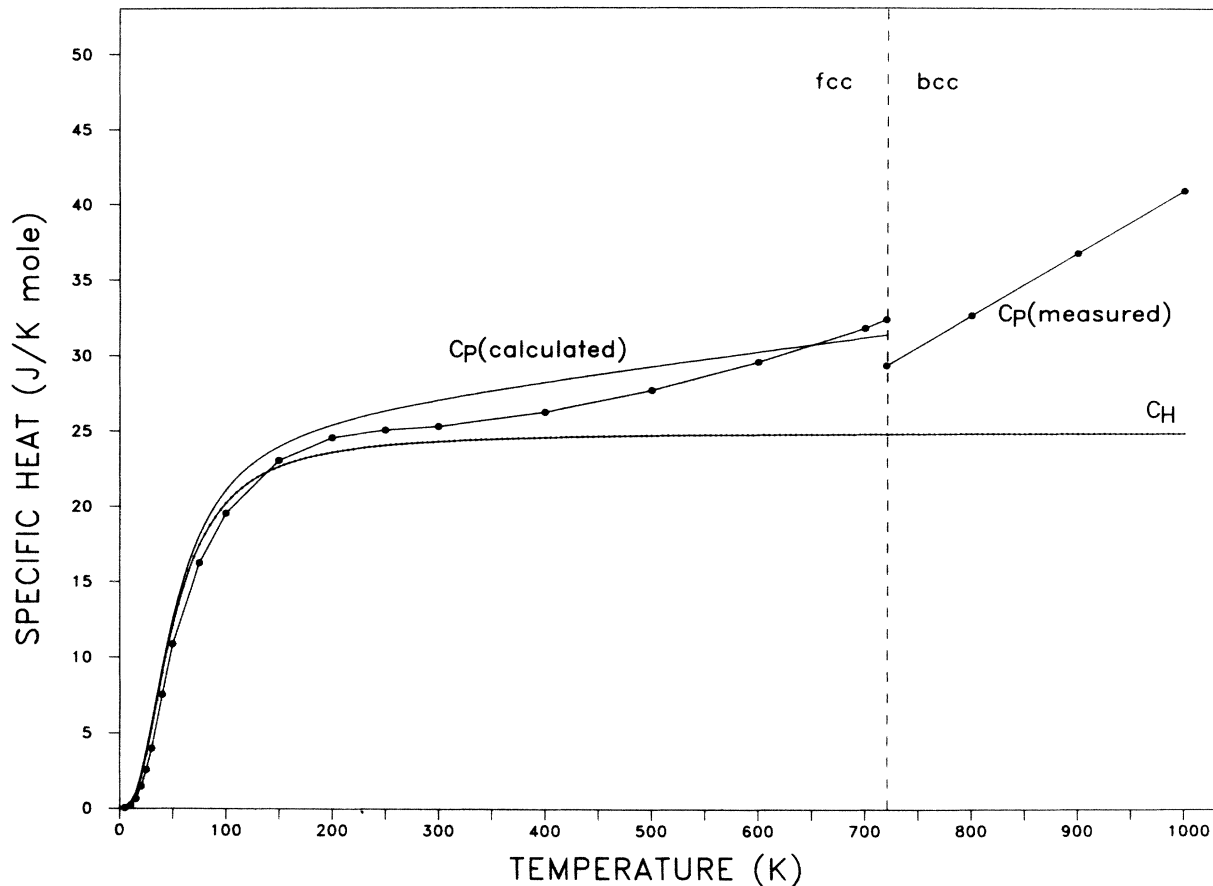


FIG. 7. Measured (—●—●—) and calculated (—) specific heat of Ca. C_H denotes the purely harmonic lattice contribution using the BvK parameters just above and below the phase transformation at 721 K.

phases. The measured values of the enthalpy difference at 721 K yield 0.70 mRy/atom (calorimetric) and 0.47 mRy/atom (vibrational entropy difference from the present work), respectively. From theoretical calculations one finds 0.7 mRy/atom (resonant pseudopotential approach by Dagens²⁷) and 1.9 mRy/atom (first-principles band-structure calculation by Skriver²⁸).

D. Pseudopotential fits

Though the Born–von Kármán model is very convenient for the parametrization of phonon dispersion curves, its great drawback is that it allows no insight into the physical nature of the forces between atoms. The two sets of Born–von Kármán parameters for the fcc and bcc phase cannot even be checked for consistency. To gain a model for both fcc and bcc phases one has to take the electronic energy into account. In simple metals this is done by plane-wave pseudopotential perturbation theory. Ca is electronically fairly simple, s - p bonded. However, the situation is somewhat complicated by the presence of an empty d band just above the Fermi level. Nevertheless, the pseudopotential approach is widely used.^{6,8,9,27,29} The predicted phonon dispersion curves vary considerably. An optimal model pseudopotential therefore has to be determined by a fit of its parameters to the experimental

phonon curves.

For our calculations we choose a model pseudopotential adequate for simple s - p metals.¹⁰ In real space it is given by

$$W_0(r) = Ze_0^2 \left[\frac{\exp(-r/r_c) - 1}{r} + \frac{a \exp(-r/r_c)}{r_c} \right], \quad (4)$$

with the free parameters a and r_c . The screening of the Fourier-transformed bare model pseudopotential was done with a dielectric function $\epsilon(q)$ given by an analytical ex-

TABLE III. Pseudopotential parameters.

Temperature (K)	With constraints			
	a	r_c (Å)	a	r_c (Å)
fcc Ca				
100			1.21	0.394
300			1.25	0.395
680	2.197	0.3102	1.22	0.434
705	2.149	0.3133	1.22	0.434
bcc Ca				
726	2.133	0.3129	1.50	0.396
750	2.283	0.3007	1.50	0.396

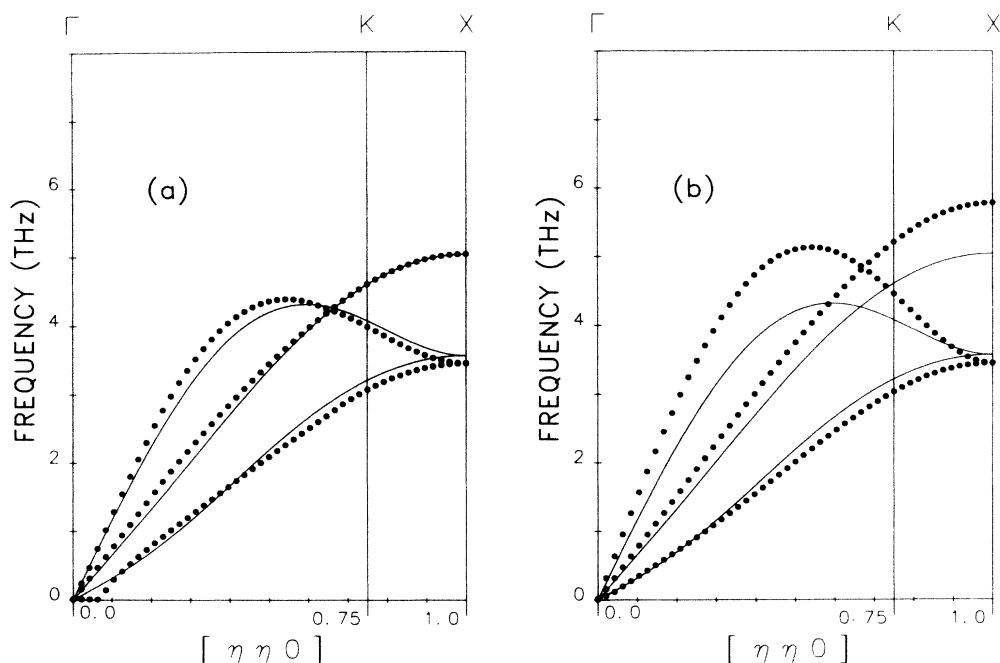


FIG. 8. Comparison of pseudopotential ($\cdot \cdot \cdot$) and BvK phonon dispersion of fcc Ca ($T = 705$ K) along $[110]$ for different pseudopotential fits (a) without constraints, (b) with c' as constraint.

pression of Ichimaru and Utsumi.³⁰ The electrostatic contribution was included by performing the Ewald transformation and summing up the terms in real and reciprocal space.³¹ In both phases, fcc and bcc, it was possible to obtain a reasonable fit of the measured data using only the two free parameters a and r_c of the pseudopotential. In the fcc case, the sum of squares of the deviations between

theory and experiment was nearly the same as the one obtained in the Born–von Kármán fit. In the bcc case, it was nearly a factor of 2 higher, which seems still reasonable in view of the small number of parameters involved. The two sets of parameters (see Table III) do in fact agree with each other within the limits of accuracy. Thus, at a first glance the pseudopotential picture seems to give a sa-

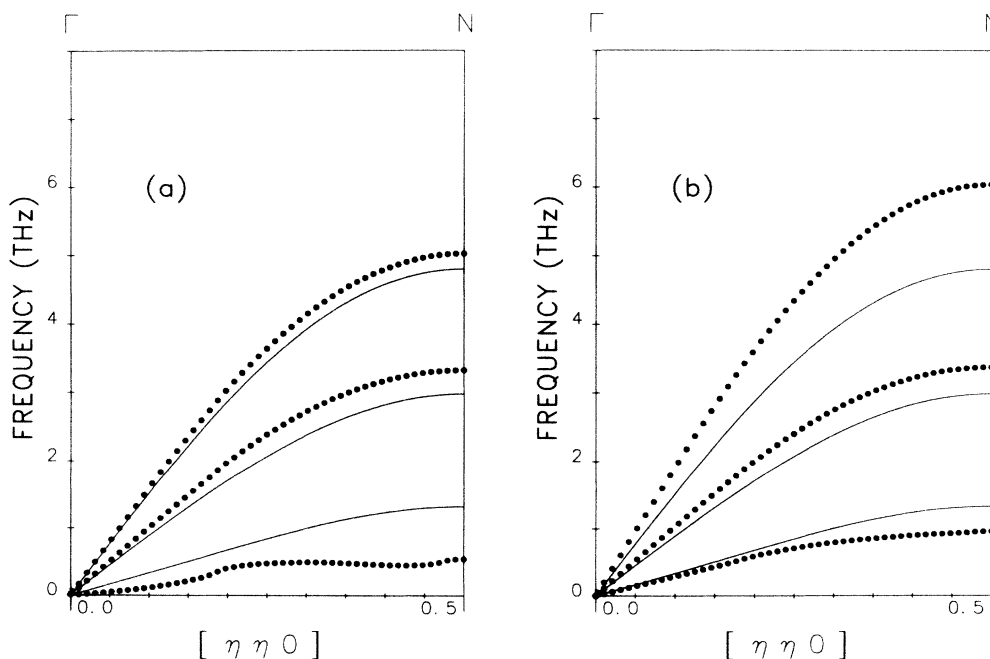


FIG. 9. Comparison of pseudopotential ($\cdot \cdot \cdot$) and BvK phonon dispersion of bcc Ca ($T = 726$ K) along $[110]$ for different pseudopotential fits (a) without constraints, (b) with c' as constraint.

tisfactory description of the phonon dispersion curves. At a closer look, however, one finds severe faults. In Figs. 8 and 9, the phonon branches along [110] obtained from the Born–von Kármán fit and from the pseudopotential fit are compared to each other. In the fcc case [Fig. 8(a)], the agreement is fairly good, but the phonon frequencies of the lower T_2 branch become imaginary at low q values in the pseudopotential picture. A fit with a different pseudopotential^{32–34} or a different screening^{35,36} gave the same result. If the stability condition is enforced by setting the measured positive c' as a constraint (c' determines the initial slope of this branch), the general agreement between the BvK and the pseudopotential results becomes much worse [Fig. 8(b)] and the sum of squares increases.

In the bcc case, even the unconstrained pseudopotential fit shows a strong deviation of the phonon frequencies of the low-lying T_2 branch. The frequencies are by more than a factor of 2 lower than the BvK frequencies. Since the zone-boundary value of this branch determines the position of the first van Hove singularity in the bcc density of states (see Fig. 6), the BvK value could be checked by a direct comparison to the data and was found to be correct. The introduction of a constraint of c' to the measured value (Table I) alleviated this discrepancy, but led to considerable deviations at the higher branches [Fig. 9(b)]. Moreover, as seen from Table III, the good agreement between fcc and bcc parameters gets lost by the constraint. On the whole, the simple pseudopotentials considered here do not give a satisfactory description of the phonons in fcc and bcc calcium. It remains to be seen whether more sophisticated approaches like the resonant model potential²⁷ or the generalized pseudopotential theory,^{18,37} which have already been applied to calculate phonons or at least elastic constants in fcc Ca, give a consistent description of the phonons in the bcc phase with the same potential parameters. In that sense, the phonon dispersion determined in the present work provides an ideal testing ground for

theoretical phonon calculations in metals with a d -electron contribution.

IV. CONCLUSIONS

Elastic constants and phonon dispersion curves have been determined for fcc and bcc calcium above and below the martensitic transformation temperature of 721 K. The results were obtained by fits of inelastic-neutron-scattering data from polycrystalline samples. The dispersion curves show no pronounced anomalies. The results for the fcc phase are in good agreement with earlier determinations.^{1,3} From the temperature dependence of the phonon frequencies, one calculates an excess specific heat which agrees fairly well with calorimetric data.

The bcc phase has a low-lying T_2 branch along the [110] direction and consequently a somewhat higher density of states at low frequencies than the fcc phase. Thus, the enthalpy favors the bcc phase at high temperatures via the vibrational entropy term. The calculated entropy difference is in quantitative agreement with that obtained from the latent heat of the martensitic phase transformation.

Within the accuracy of the measurements (about 5% for the phonon frequencies), no precursor effects or mode softening could be discovered, neither in the elastic constant c' nor in any of the zone-boundary modes.^{19,20} Though a fit with the same pseudopotential in both phases could reproduce the general features of the phonon dispersion, there are considerable deviations at some phonon branches, especially at low frequencies. In the fcc phase there is even a violation of the stability condition. Since this result was obtained for different pseudopotentials, we conclude that the local pseudopotential picture is too simple for Ca and therefore cannot be used as a semi-empirical tool to extrapolate from one structure to another.

*This work is part of the Ph.D. thesis of M. Heiroth at the University of Düsseldorf.

¹U. Buchenau, M. Heiroth, H. R. Schober, J. Evers, and G. Oehlinger, *Phys. Rev. B* **30**, 3502 (1984).

²U. Buchenau, H. R. Schober, and R. Wagner, *J. Phys. (Paris) Colloq.* **42**, C6-395 (1981).

³C. Stassis, J. Zaretsky, D. K. Misemer, H. L. Skriver, B. N. Harmon, and R. M. Nicklow, *Phys. Rev. B* **27**, 3303 (1983).

⁴J. Mizuki, Y. Chen, K.-M. Ho, and C. Stassis, *Phys. Rev. B* **32**, 66 (1985).

⁵V. Heine and D. Weaire, in *Solid State Physics*, edited by H. Ehrenreich, F. Seitz, and D. Turnbull (Academic, New York, 1970), Vol. 24, p. 250.

⁶A. O. E. Animalu, *Phys. Rev.* **161**, 445 (1967).

⁷J.-P. Jan and H. L. Skriver, *J. Phys. F* **11**, 805 (1981).

⁸M. V. N. Ambika Prasad, H. C. Gupta, and B. B. Tripathi, *Phys. Rev. B* **29**, 3708 (1984).

⁹H. C. Gupta, G. S. Reddy, Vijai Baboo Gupta, and B. B. Tripathi, *Phys. Rev. B* **33**, 5839 (1986).

¹⁰G. L. Krasko, Z. A. Gurskii, *Pis'ma Zh. Eksp. Teor. Fiz.* **9**, 596 (1969) [*JETP Lett.* **9**, 363 (1969)].

¹¹J. Evers, G. Oehlinger, A. Weiss, C. Probst, M. Schmidt, and P. Schramel, *J. Less-Common Met.* **81**, 15 (1981).

¹²U. Buchenau, *Solid State Commun.* **32**, 1329 (1978).

¹³S. N. Vaidya and G. C. Kennedy, *J. Phys. Chem. Solids* **31**, 2329 (1970).

¹⁴E. C. Bain, *Trans. Am. Inst. Min. Metall. Pet. Eng.* **70**, 25 (1924).

¹⁵P. F. Gobin and G. Guenin, in *Solid State Phase Transformations in Metals and Alloys*, edited by D. de Fontaine (Editions de Physique, Orsay, 1979), p. 573.

¹⁶N. Nakanishi, A. Nagasawa, and Y. Murakami, *J. Phys. (Paris) Colloq.* **43**, C4-35 (1982).

¹⁷U. Buchenau, H. R. Schober, J. M. Welter, G. Arnold, and R. Wagner, *Phys. Rev. B* **27**, 955 (1983).

¹⁸J. A. Moriarty, *Phys. Rev. B* **28**, 4818 (1983).

¹⁹G. Ernst, C. Artner, O. Blaschko, and G. Krexner (private communication).

- ²⁰O. Blaschko and G. Krexner, Phys. Rev. B **30**, 1667 (1984).
- ²¹J. Mizuki and C. Stassis, Phys. Rev. B **32**, 8372 (1985).
- ²²Y. Chen, K.-M. Ho, B. N. Harmon, and C. Stassis, Phys. Rev. B **33**, 3684 (1986).
- ²³G. Gilat and L. J. Raubenheimer, Phys. Rev. **144**, 390 (1966).
- ²⁴J. C. K. Hui and P. B. Allen, J. Phys. C **8**, 2923 (1975).
- ²⁵R. Hultgren, P. D. Desai, D. T. Hawkins, M. Gleiser, K. K. Kelley, and D. D. Wagman, *Selected Values of the Thermodynamic Properties of the Elements* (American Society for Metals, Metals Park, Ohio, 1973), p. 99, and further references therein.
- ²⁶B. T. Bernstein and J. F. Smith, Acta Crystallogr. **12**, 419 (1959).
- ²⁷L. Dagens, J. Phys. F **7**, 1167 (1977).
- ²⁸H. L. Skriver, Phys. Rev. B **31**, 1909 (1985).
- ²⁹K. S. Sharma and C. M. Kachhava, Solid State Commun. **38**, 1083 (1981); K. S. Sharma, Phys. Status Solid B **108**, K101 (1981); M. Taut and H. Eschrig, *ibid.* **73**, 151 (1976).
- ³⁰S. Ichimaru and K. Utsumi, Phys. Rev. B **24**, 7385 (1981).
- ³¹M. L. Cohen and V. Heine, in *Solid State Physics*, edited by H. Ehrenreich, F. Seitz, and D. Turnbull (Academic, New York, 1970), Vol. 24, p. 37.
- ³²N. W. Ashcroft, Phys. Lett. **23**, 48 (1966).
- ³³W. A. Harrison, *Pseudopotentials in the Theory of Metals* (Benjamin, New York, 1966).
- ³⁴S. Nand, B. B. Tripathi, and H. C. Gupta, J. Phys. Soc. Jpn. **41**, 1237 (1976).
- ³⁵J. Lindhard, K. Dan. Vidensk. Selsk. Mat.-Fys. Medd. **28**, 8 (1954).
- ³⁶Dielectric function of Geldart and Vosko according to D. L. Price, K. S. Singwi, and M. P. Tosi, Phys. Rev. B **2**, 2983 (1970).
- ³⁷J. A. Moriarty, Phys. Rev. B **6**, 4445 (1972); **8**, 1338 (1973); **26**, 1754 (1982).